



PX No. 176

BNL 66669

Filename: 19845.pdf

**Measuring Global Observables with PHENIX**

M.J. Bennett for the  
PHENIX Collaboration

**Workshop on Particle Distributions  
In Hadronic and Nuclear Collisions,  
University of Illinois, June 12, 1998**

Physics Department

Brookhaven National Laboratory  
Operated by  
Brookhaven Science Associates  
Upton, NY 11973

Under Contract with the United States Department of Energy  
Contract Number DE-AC02-98CH10886

# MEASURING GLOBAL OBSERVABLES WITH PHENIX<sup>a</sup>

M. J. BENNETT, FOR THE PHENIX COLLABORATION

*Physics Division, P-25, MS H846*

*Los Alamos National Laboratory, Los Alamos*

*NM 87545, USA*

*E-mail: mjbennett@lanl.gov*

PHENIX is a multi-purpose spectrometer which will be capable of measuring hadrons, photons and leptons produced in collisions of ultra-relativistic nuclei at the Relativistic Heavy-Ion Collider (RHIC). The capability of PHENIX to measure various global aspects of the collision, *i.e.* charged particle multiplicity, transverse energy and mean transverse momentum of produced particles, will be discussed, as well as the importance of these measurements to the overall PHENIX physics program.

## 1 The PHENIX Experiment

### 1.1 Introduction

When the Relativistic Heavy-Ion Collider (RHIC) begins operations, it will be capable of colliding nuclei of various sizes, from protons up to Au, at center-of-mass energies of 200 to 500 GeV per nucleon pair. Some of these collisions are expected to produce a new state of matter, the quark-gluon plasma (QGP), in which quarks are no longer confined to individual hadrons and in which chiral symmetry has been restored. Numerous predictions have been made as to how a phase transition to a QGP would affect the particle spectra produced in these collisions (see, for example, a recent review by Harris and Müller<sup>1</sup>).

The PHENIX physics philosophy is to detect and systematically study the QGP via a simultaneous measurement of many different probes/signatures of the plasma, as a function of the energy density achieved in the nucleus-nucleus collision. To achieve this goal, the PHENIX detector has been designed as a multi-purpose spectrometer, capable of concurrently measuring hadrons, leptons and photons, as well as global properties of the collision, *e.g.* energy density, as will be detailed below.

### 1.2 The PHENIX Detector

The PHENIX detector, which has been described in detail elsewhere<sup>2</sup>, is shown in Fig. 1; the various major subsystems of the detector are individually labelled.

---

<sup>a</sup>Proceedings of an invited talk at the Univ. of Illinois-Chicago Workshop on Particle Distributions in Hadronic and Nuclear Collisions, June 11-13, 1998.

In this diagram, the beams enter from the sides, with collisions occurring within the Multiplicity/Vertex Detector (MVD), a large acceptance charged particle detector which is described in detail in Sec. 2.2. The time of the interaction is determined by two Cherenkov-based Beam-Beam counters surrounding the beam pipes both upstream and downstream of the interaction region, which measure high pseudo-rapidity charged particles from the interaction. There are four spectrometer “arms”—two in the central rapidity region, each covering  $90^\circ$  in azimuth, and two arms for detecting muons at higher rapidities.

The central rapidity arms cover the pseudorapidity range  $-0.35 \leq \eta \leq 0.35$ , and allow for the measurement of  $d^2N/d\eta dp_t$  for identified hadrons;  $\pi/K$  separation can be achieved up to  $p_t=2.5$  GeV/ $c$  for the  $30^\circ$  of azimuth covered by a high-resolution time-of-flight detector, and up to  $p_t=1.4$  GeV/ $c$  for the rest of the azimuthal coverage, using time-of-flight information from the Electromagnetic Calorimeter (EMCal). The difficult task of identifying the relatively few electrons amongst the huge number of pions produced is accomplished by combining the reconstructed momentum with information from a Ring-Imaging Cherenkov detector (RICH), energy deposition in the EMCal and  $dE/dx$  in the Time-Expansion Chamber; taking all this information together, a pion rejection factor of greater than  $10^4$  is expected for electrons in the central arms. Finally, photon energies can be measured using the EMCal, which will allow the measurement of  $\pi^0$  and  $\eta$  spectra; an upper limit of  $\sim 40$  GeV in photon energy will also allow the study of jets (via leading  $\pi^0$ ,  $\eta$ ) in the plasma.

The versatility of the PHENIX detector allows for a very broad physics program, including most of the proposed QGP signatures. PHENIX will investigate the possibility of a chiral phase transition via: a shift in the  $\phi$  mass and a change in the relative branching ratio between  $\phi \rightarrow e^+e^-$  and  $\phi \rightarrow K^+K^-$ ; enhanced strangeness through the  $K/\pi$  ratio; enhanced production of antinuclei, and other topics. The deconfinement transition can be sought by measuring: suppression of charmonium production brought about by Debye screening (see M. Rosati’s paper in these proceedings); lepton pairs below  $\sim 3$  GeV/ $c$  resulting from  $q\bar{q}$  annihilation in a deconfined plasma; direct photons in the energy range between 2 and 5 GeV from  $gq \rightarrow \gamma q$  Compton scattering; jet quenching from an increased  $dE/dx$  of quarks traversing the QGP, and other topics. For each of these processes, the most convincing evidence of a QGP transition would be a change, perhaps an abrupt change, in the systematic behavior of the process with increasing event centrality. The evidence would be even more compelling if changes were seen in multiple signature channels at the same point in event centrality. In order to observe whether or not this sort of behavior occurs, it is important for PHENIX to simultaneously measure not only numerous proposed signatures, but also the global characteristics of the

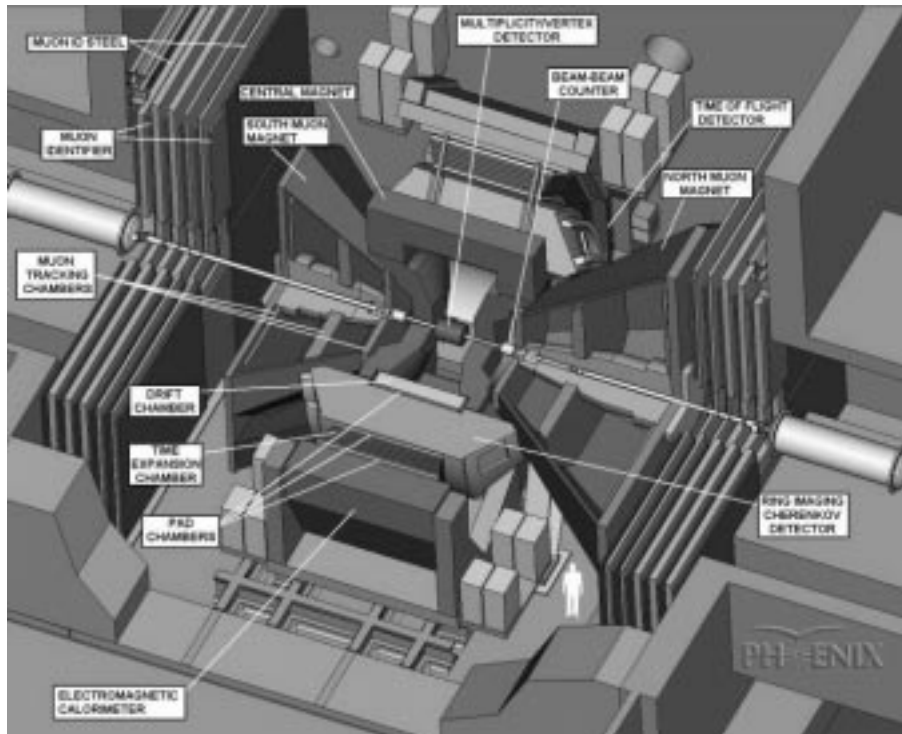


Figure 1: Cutaway schematic diagram of the PHENIX apparatus.

collisions.

## 2 Global Observables

### 2.1 Physics Motivation

PHENIX will measure several quantities which are considered “global observables”, *i.e.* quantities which describe the overall dynamics of the collision, including charged particle multiplicity ( $dN_{ch}/d\eta$ ), transverse energy ( $dE_t/d\eta$ ), mean transverse momentum ( $\langle p_t \rangle$ ) of produced hadrons, and the number of spectator neutrons ( $N_{spect}$ ).<sup>b</sup> These quantities are inherently of great interest,

<sup>b</sup>The measurement of  $N_{spect}$  will be accomplished using a zero-degree hadron calorimeter. Detectors of identical design will be utilized by all of the RHIC experiments; the details will not be discussed here. Of the measured global quantities,  $N_{spect}$  is the most directly related

providing valuable information regarding the dynamics of nucleus-nucleus collisions at RHIC energies, including such important issues as baryon stopping, longitudinal and transverse flow, temperature of the collision region, *etc.* Investigating the mean behavior of  $dN_{ch}/d\eta$  and  $dE_t/d\eta$  as a function of  $N_{spect}$  should lead to a better understanding of energy deposition and subsequent particle production in the interaction region.

It should be noted that the measurement of global event characteristics will be some of the first results from PHENIX. Currently, cascade-type models for describing  $A-A$  collisions at RHIC (*e.g.* VNI, HIJING, HIJET, RQMD) differ by factors of 2 or more in the magnitude of their predicted  $dN_{ch}/d\eta$  spectra; the shapes of the predicted spectra are also significantly different. To a large extent these discrepancies can be attributed to uncertainties in extrapolation—either in energy scaling of measurements made at the much lower energies available at the CERN-SPS ( $\sqrt{s} \sim 20$  GeV per nucleon pair) and the BNL-AGS ( $\sqrt{s} \sim 5$  GeV per nucleon pair) to RHIC energies ( $\sqrt{s}=200$  GeV per nucleon pair); or in extrapolation from  $p-p$  interactions at similar energies to the much more complicated  $A-A$  system. Similarly, predictions of hydrodynamic models vary greatly, depending on the assumptions made concerning the initial conditions of the fireball<sup>3</sup>. Early measurements of the actual global distributions will significantly constrain the models. These constraints will be important not just in understanding the global collision dynamics *per se*, but also in providing a relevant framework for predictions of other quantities which depend on the detailed dynamics of the collision, *e.g.*  $J/\psi$  suppression.

There are also proposed QGP signatures which can be directly investigated with global measurements. Large fluctuations in  $dN_{ch}/d\eta$  and  $dE_t/d\eta$  as a function of  $N_{spect}$  could indicate the formation of QGP droplets within an otherwise hadronic interaction region. Additionally, event-by-event fluctuations of  $dN_{ch}/d\eta$ , localized in particular regions of phase space, could indicate the formation of a disoriented chiral condensate (DCC), which would be a signature of chiral symmetry restoration. Finally, it has been proposed that a large increase in entropy associated with a deconfinement transition could manifest itself in a significant increase in  $\langle p_t \rangle$  for hadrons.

As the PHENIX physics program matures, probably the most significant role of global event measurements will be as a means to study the systematic behavior of various proposed QGP signatures, *e.g.* as a function of the energy density achieved in the collisions. Energy density ( $\varepsilon$ ) can be inferred from

---

to the geometry of the collision and the least sensitive to the physics of the interaction region, and thus provides an unbiased yardstick for examining the behavior of the other global observables.

actual measured quantities using the Bjorken formalism<sup>4</sup>:

$$\varepsilon \approx \frac{1}{\pi R_T^2 \tau_0} \frac{dE_t}{dy} \approx \frac{1}{\pi R_T^2 \tau_0} \sqrt{\langle p_t^2 \rangle + m_\pi^2} \frac{dN_\pi}{dy} \quad (1)$$

where  $\tau_0$  is the freeze-out time (nominally assumed to be  $\sim 1$  fm/c) and  $R_T$  is the size of the system at time  $t=\tau_0$ .

## 2.2 Charged Particle Multiplicity

In PHENIX, charged particle multiplicity,  $dN_{ch}/d\eta$ , will primarily be measured using the Multiplicity/Vertex Detector (MVD), which is shown in Fig. 2. The detector system incorporates a clamshell design, which encloses the beam pipe. There are two hexagonal barrels of Si microstrip detectors, at  $\sim 5$  cm and  $\sim 7.5$  cm from the center of the beam pipe. The inner barrel is fully populated, comprising a total of 72 Si detectors, separated into a segmentation of 6 azimuthally and 12 along the beam direction; for the outer barrel only 2 of the 6 azimuthal sections are fully populated, with the central portion of the other 4 azimuthal sections left empty to reduce the mass of the detector in the acceptance of the central arms. Altogether, there are 112 Si strip detectors, each of which contains 256 microstrips at a  $200 \mu\text{m}$  pitch, oriented perpendicularly to the beam, as shown in Fig. 2. The endcaps of the detector each contain 12 Si pad detectors, spanning the radial distance from  $\sim 5$  to  $\sim 12$  cm from the center of the beam pipe. Each of these detectors contains 252 square Si pads, which range in area from  $4 \text{ mm}^2$  to  $\sim 20 \text{ mm}^2$ ; the dimensions were chosen so that each pad covers  $\Delta\eta=0.04$  and  $\Delta\varphi \sim 2.5^\circ$  (for interactions at the center of the detector). All told the MVD comprises just under 35,000 channels.

The MVD has excellent acceptance, with the strip detectors covering  $-2.5 \leq \eta \leq 2.5$  and the pad detectors covering  $1.8 \leq |\eta| \leq 2.65$  for interactions at the center of the MVD (the exact  $\eta$  range depends on the position of the interaction); for most of the  $\eta$  range, the MVD covers the full range in azimuth. The design employs very high segmentation in the  $\eta$  dimension for the strip detectors, which allows for an accurate determination of the vertex position (simulated longitudinal vertex position resolution for central Au+Au events is a few hundred microns); the segmentation is high in both the  $\eta$  and  $\varphi$  dimensions for the pad detectors, which should allow a sensitive search for localized fluctuations in  $dN_{ch}/d\eta d\varphi$ . High segmentation is also necessary to keep occupancy levels at a reasonable level; for central Au+Au HIJING events (midrapidity  $dN_{ch}/d\eta \sim 800$ ), the occupancy is approximately 50% in the strip detector barrels, and 10-15% for the pad detectors. Thus, the probability of

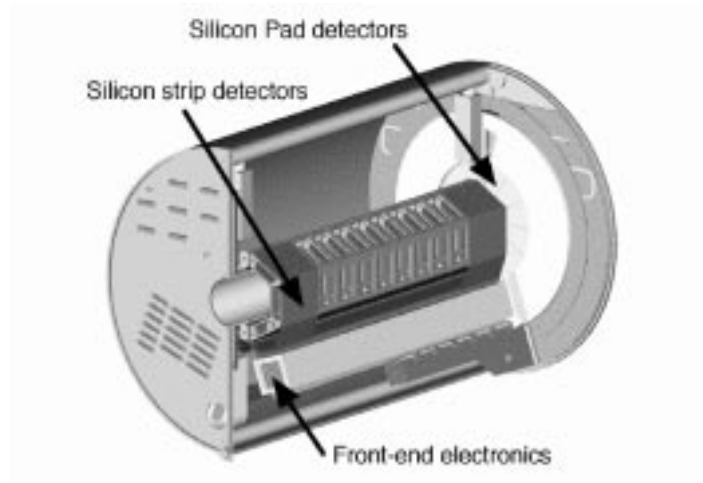


Figure 2: Cutaway diagram of the PHENIX Multiplicity/Vertex Detector. The active area includes two concentric barrels of Si microstrip detectors and two endcaps containing Si pad detectors.

multiple hits in a given strip is fairly high, although less so for the pad detectors. It should be noted that some event generators, *e.g.* VNI, predict multiplicities around twice as high as HIJING. The MVD electronics will be adjusted such that the average energy deposition of a single minimum ionizing particle (MIP) will be  $\sim 1/8$  full scale of the ADC's; thus, the MVD should be able to make a reasonable  $dN_{ch}/d\eta$  measurement at multiplicities considerably higher than predicted values, although certainly things become more complicated as the occupancy becomes very high.

In order to make an accurate measurement of  $dN_{ch}/d\eta$  in the case of high occupancy, there must exist a strategy for discerning multiple particle hits from Landau fluctuations in the energy deposition of a single particle. In the MVD analysis software, there are two different approaches for dealing with this problem. In the case of the strip detectors, the approach is to reduce the impact of Landau fluctuations by averaging over “clumps” of strips. Individual strip ADC's are gain-corrected and adjusted for path length in the Si (based on reconstructed vertex position), then summed over a clump; this sum is then normalized by the average MIP energy deposition to get the number of hits in the clump. The clump size is an adjustable parameter, with a nominal value of 64. For the pad detectors, a different approach is used: ADC values for individual pads are first gain-corrected and adjusted for path length in the Si,

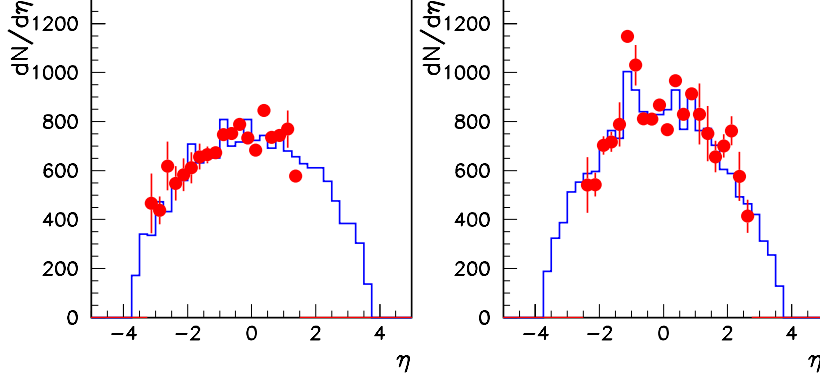


Figure 3: A comparison of  $dN_{ch}/d\eta$  distributions from single HIJING Au+Au central events (shown as histograms) to the expected response of the MVD (shown as symbols), from two sample events chosen randomly.

then normalized by the average MIP value. The number of hits ( $N_{hit}$ ) for each pad is then assigned based on a weighted expectation value:

$$N_{hit} = \frac{\sum_{n=1}^{N_{max}} n P_n(ADC) P_n(occupancy)}{\sum_{n=1}^{N_{max}} P_n(ADC) P_n(occupancy)} \quad (2)$$

where  $P_n(ADC)$  is the probability that  $n$  hits will result in a given ADC value, as determined by randomly adding a calibration ADC distribution from known single hits  $n$  times, and  $P_n(occupancy)$  is the likelihood of  $n$  hits in a given pad, determined by Poisson statistics and the overall occupancy in the pad detectors. Since the determination of  $P_n(occupancy)$  requires a knowledge of  $N_{hit}$ , these two quantities are calculated in a two-step iterative process, with the initial pass assuming  $N_{hit}=1$  for all pads. This approach returns a non-integer value for the number of hits in a given pad. It is also possible to use a clumping approach for the pads, which yields similar performance.

The response of the MVD to HIJING and HIJET events has been simulated, including effects of background particles from interactions in detector material, as well as crosstalk and electronic noise, estimated from prototype tests. Averaged over 125 central Au+Au HIJET events, the mean  $dN_{ch}/d\eta$  from the MVD simulation (using bins of  $\Delta\eta=0.25$ ) was within a few percent of



the actual input mean  $dN_{ch}/d\eta$ . The  $dN_{ch}/d\eta$  resolution of the MVD for single HIJET events is shown in Fig. 3. The simulated measurement is very close to the actual values, including those bins where there are statistical fluctuations. These simulations bode well for the prospect of using the MVD to look for physics-related fluctuations in  $dN_{ch}/d\eta$ . Both the high segmentation of the detector and the algorithms used to calculate  $dN_{ch}/d\eta$  naturally lend themselves to multi-dimensional studies, *e.g.* wavelet analyses, which are powerful tools for detecting fluctuations.

### 2.3 Transverse Energy

Transverse energy distributions ( $dE_t/d\eta$ ) will primarily be measured with an electromagnetic calorimeter (EMCal), the outermost detector in the central rapidity arms, sitting at a radial distance of  $\sim 5$  m from the interaction point. PHENIX will utilize two different technologies for the EMCal:  $135^\circ$  of azimuthal coverage will be with a lead-scintillator (PbSc) “shish-kebab” sampling calorimeter, while the remaining  $45^\circ$  of azimuthal coverage will utilize Pb-glass Cherenkov detectors. Both types of detectors cover the full  $\eta$  range of the central arms,  $-0.35 \leq \eta \leq 0.35$ .

The fundamental unit of the PbSc part of the EMCal is a module, as shown in Fig. 4. Each module has four independent towers, each of which consists of a 66-layer Pb-scintillator sandwich stack, threaded by wavelength shifting fibers which carry the scintillator light back to a photomultiplier tube. Towers are 5.25 cm square at the front face and 37 cm deep. The Pb-glass portion of EMCal is constructed of modules, each of which are 4 cm square at the front face and 40 cm deep. Altogether, there are in excess of 28,000 channels in the EMCal. The high segmentation leads to a reasonable occupancy; even for  $dN/d\eta \sim 1500$ , the estimated probability that a given particle is isolated within a  $2 \times 2$  cell matrix is 85%.

Both EMCal technologies have been thoroughly tested—the PbSc in beam tests at Brookhaven, and the Pb-glass as part of the WA98 experiment at the CERN-SPS. Both have been found to have excellent energy resolution, with  $7.8\%/\sqrt{E} \oplus 1.5\%$  for the PbSc and  $5.8\%/\sqrt{E} \oplus 1.0\%$  for the Pb-glass. The PbSc also has good timing resolution at 280 ps, which will aid in particle identification. Both detector types are optimized for electromagnetic response (with a depth of 18-20 radiation lengths); the mean straight-through energy deposition for charged hadrons is 225 MeV for PbSc and 500 MeV for Pb-glass.

Recently, simulations have been performed of the EMCal  $dE_t/d\eta$  measurement<sup>5</sup>. As expected, the response for neutral energy (mostly from  $\pi^0 \rightarrow \gamma\gamma$ ) was very good, with the total reconstructed transverse energy from photons

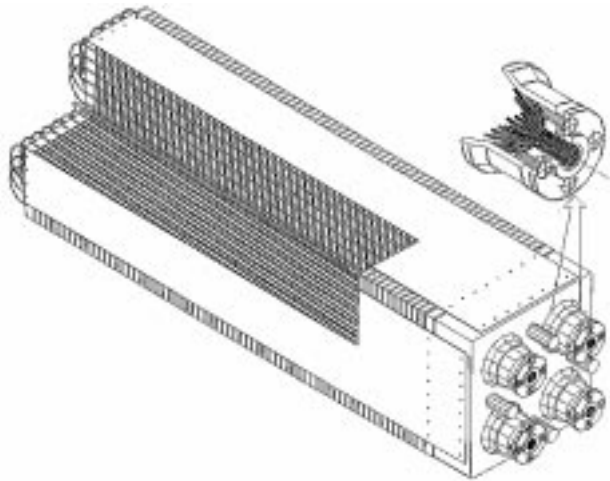


Figure 4: Schematic diagram of a single PbSc module, consisting of four towers. The design is “shish-kebab” style; the active area, consisting of a 66-layer lead/scintillator stack, is threaded by wave-length shifting fibers, which carry the scintillator light to photomultiplier tubes at the end.

representing 93% of that in the EMCal acceptance from the event generator. The background contribution from non-vertex related particles (this includes both decays in flight as well as particles generated by interactions in detector material) was  $\sim 35\%$ , and was largely independent of impact parameter. By applying a random event-by-event background correction based on the mean background distribution, the actual input  $dE_t/d\eta$  was reproduced quite well, with a resolution of around 4%.

#### 2.4 Mean Transverse Momentum

The tracking portions of the central rapidity arms are designed to measure the momentum of all charged particles originating from the interaction vertex and falling within their acceptance of  $\Delta\eta=0.7$  and  $\Delta\varphi=2 \times 90^\circ$ . Trajectory information comes from sets of drift chambers and pad chambers, a time-expansion chamber and EMCal; combined with the known magnetic field, the particle’s rigidity can be inferred. Particle identification, as described in Sect. 1.2, allows for measuring single charged particle  $d^2N/d\eta dp_t$  spectra; this information also gives  $dN_{ch}/d\eta$  and  $dE_t/d\eta$  measurements which supplement those made by the MVD and the EMCal alone. Single particle  $d^2N/d\eta dp_t$  for  $\pi^\circ$  will be available by reconstructing photon pairs in the EMCal. The single

particle spectra are interesting in their own right, and will also allow PHENIX to perform other analyses, *e.g.* particle correlations, flow studies through  $p_t$  distributions as a function of mass, *etc.*

The occupancy of the central rapidity arms is quite high, with around 300 charged tracks in each arm for a central Au+Au HIJING event. The track finding efficiency is expected to be  $\sim 90\%$ . To reduce computing time, momentum reconstruction will be done via interpolation using a highly segmented lookup table. Simulations indicate that the inherent loss of resolution incurred by using a table is considerably less than the multiple scattering limit. Averaged over all phase space, momentum resolution for charged particles is expected to be  $\sim 1\%$ . Thus, PHENIX should be able to make a very accurate measurement of the  $p_t$  spectra for hadrons.

### 3 Summary

PHENIX has a robust physics program for measuring the global aspects of heavy ion collisions at RHIC, including  $dN_{ch}/d\eta$ ,  $dE_t/d\eta$  and  $\langle p_t \rangle$  for hadrons. These quantities should be among the first physics to come out of RHIC, and will be integral to understanding the collision dynamics at these energies. PHENIX measures a number of proposed QGP signatures concurrently with the global properties of the collisions, allowing investigation of the systematic behavior of the signature processes, which will be essential to our understanding of the QGP phase transition.

### Acknowledgments

Construction of the PHENIX detector has been supported by the Department of Energy (USA), Monbu-sho and STA (Japan), RAS, RMAE, and RMS (Russia), BMBF (Germany), FRN and the Knut & Alice Wallenberg Foundation (Sweden), and MIST and NSERC (Canada).

### References

1. J.W. Harris and B. Müller, *Annual Reviews of Nuclear and Particle Science* **46**, 71 (1996).
2. PHENIX Conceptual Design Report, BNL 1993 (unpublished).
3. B.R. Schlei and D. Strottman, LANL Preprint nucl-th/9806034.
4. J.D. Bjorken, *Phys. Rev. D* **27**, 140 (1983).
5. V. Bumazhnov *et al*, PHENIX-EMC Technical Note (in preparation), 1998.